Photochemistry and Photobiology, 1999, 69(4): 429–434

Ground- and Excited-State Characterization of an Electrostatic Complex between Tetrakis-(4-Sulfonatophenyl)porphyrin and 16-Pyrimidinium Crown-4

Randy W. Larsen*[1], Michael K. Helms[2], W. Russell Everett[1] and David M. Jameson[2]

Departments of [1]Chemistry and [2]Genetics and Molecular Biology, University of Hawaii at Manoa, Honolulu, HI, USA

Received 9 April 1998; accepted 22 December 1998

ABSTRACT

We report the formation of an electrostatic complex between (16-pyrimidinium crown-4)tetranitrate (16PC4) and tetrakis-(4-sulfonatophenyl)porphyrin (4SP) in aqueous solution. Ground-state complex formation results in a red shift of the 4SP visible absorption bands and a decrease in absorbance of the Soret band. The equilibrium constant for complex formation (determined from optical titrations) is found to be (2.0 ± 0.2) × 10^5 M^{-1}. In addition, the data fit to an expression describing a 1:1 stoichiometry. Excitation of the complex results in quenching of both the excited singlet and triplet states of the associated porphyrin. The singlet-state lifetime decreases from 10 ns for the free porphyrin to 1.5 ns in the presence of 16PC4 at low solution ionic strengths. In addition, evidence is presented for triplet-state quenching within the complex with k_q = (1.1 ± 0.1) × 10^4 s^{-1}. The mechanism of quenching is tentatively assigned to electron transfer from either the excited singlet or excited triplet state of the porphyrin to the ground state of the 16PC4.

INTRODUCTION

Biological electron transfer (ET)† reactions occur between electrostatically stabilized protein : protein complexes and between various redox-active cofactors embedded within a single protein complex. In general, intermolecular ET rates are modulated by donor–acceptor distance, thermodynamic driving force, donor–acceptor orientation, the nature of the intervening medium and both inner-sphere and outer-sphere reorganization (1–8). Additional mechanistic steps include (1) formation of the protein : protein complex, (2) ET between the redox centers of each protein within the complex and (3) dissociation of the protein : protein complex. Thus, the rate of ET in such complexes may have an additional component to the overall reorganizational energy required for intermolecular ET that influences protein : protein recognition and docking (*i.e.* gating effects) (9–15). Unfortunately, the complexity of protein : protein ET reactions makes detailed understanding of this fundamentally important process extremely difficult.

Considerable attention is now being focused on the development of model systems that share similar properties to protein : protein ET reactions including self-assembly and molecular recognition. Model systems have been developed that couple self-assembly and molecular recognition driven by hydrogen-bond interactions, electrostatic attractions and hydrophobic interactions with photoactive donor/acceptor molecules to probe ET reactions through noncovalent pathways (16–21). Recent studies by Jasuja *et al.* (22) and Larsen *et al.* (23,24) have demonstrated the importance of conformational dynamics and donor/acceptor orientation in the modulation of ET rates within several photoactive noncovalent complexes (both small molecule : small molecule and protein : small molecule complexes). The observed conformational dynamics are governed by the nature of the interface between the donor and the acceptor.

In our continued efforts to understand the dynamics of intermolecular ET we have developed a new model system involving the photoactive anionic porphyrin (tetrakis-[4-sulfonatophenyl]porphyrin [4SP]) and the cationic macrocycle (16-pyrimidinium crown-4)tetranitrate (16PC4) (see Fig. 1 for structural diagrams). This system is similar to supramolecular complexes involving 4SP/18-crown-6, 4SP/[32]ane-$N_8H_8^{8+}$, hexacyanocobaltate(III)/[32]ane-$N_8H_8^{8+}$ and Ru(bpy)$(CN)_4^{2-}$/[32]ane-$N_8H_8^{8+}$ (25–28). Our data reveal ionic strength-dependent complexation and porphyrin singlet- and triplet-state quenching in the presence of 16PC4. Preliminary cyclic voltametry studies of the 16PC4 suggest that the mechanism of quenching is ET from the excited-state porphyrin to the 16PC4 within the complex. The fact that ET is observed from both singlet and triplet states of the porphyrin within the complex suggests equilibrium orientational/conformational differences within the self-associated complex.

MATERIALS AND METHODS

The 16PC4 was prepared using methods described previously (29). The 4SP and tertakis(*N*-methylpyridyl)porphyrin (T4MPYP) were purchased from Porphyrin Products (Logan, UT) and used

*To whom correspondence should be addressed at: Department of Chemistry, University of Hawaii at Manoa, Honolulu, HI 96822, USA. Fax: 808-956-5908; e-mail: rlarsen@gold.chem.hawaii.edu

†*Abbreviations*: ET, electron transfer; 4SP, tetrakis-(4-sulfonatophenyl)porphyrin; ^{1}P, porphyrin singlet state; ^{3}P, porphyrin triplet state; 16PC4, 16-pyrimidinium crown-4)tetranitrate; T4MPYP, tetrakis(*N*-methylpyridyl)porphyrin.

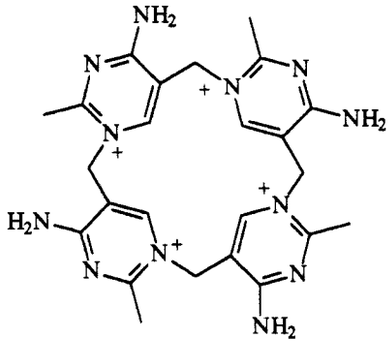

16-Pyrimidinium crown-4

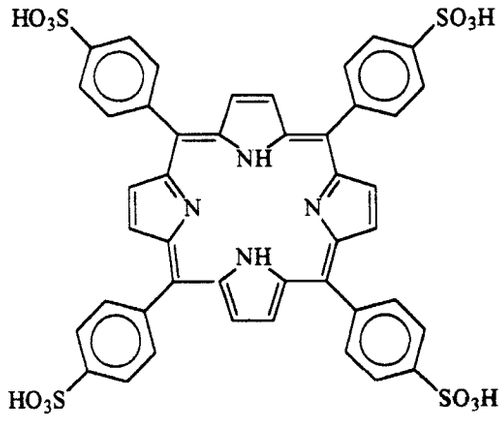

Tetrakis-(4-sulphonatophenyl)Porphyrin

Figure 1. Structural diagram of 16PC4 (top) and 4SP (bottom).

without further purification. The 16PC4, T4MPYP and 4SP were prepared as stock solutions in water (16PC4 and T4MPYP) and 0.1 *N* NaOH (4SP). Stock solution concentrations (~20 m*M* and ~3 m*M* for 16PC4 and 4SP/T4MPYP, respectively) were determined using ϵ_{256nm} = 71.4 mM^{-1} cm^{-1} (16PC4) (determined as part of this work), ϵ_{516nm} = 16 mM^{-1} cm^{-1} (4SP) and ϵ_{518nm} = 29.8 mM^{-1} cm^{-1} (T4MPYP) (30). Steady-state absorption spectra were obtained using a Milton-Roy Spectronic 3000 diode-array spectrophotometer.

Nanosecond transient absorption studies were carried out using instrumentation described previously (31). Briefly, samples were excited with a 532 nm laser pulse (7 ns, 3 mJ/pulse) from a frequency-doubled Nd:YAG laser (Continuum Sure Lite II). The change in absorbance was monitored by focusing the arc of a 150 W Xe-arc lamp (Oriel) through the sample and overlapping with the laser pulse. The light passing through the sample was then imaged onto the entrance slit of a Spex 1680B 1/4 M double monochrometer and detected using a thermoelectrically cooled photomultiplier tube (Hamamatsu, R928). The transient signal was then amplified using electronics of our own design and recorded using a Tektronix RTD710A 200 MHz transient digitizer. The data were transferred and manipulated with an IBM-based 486PC. The transient absorption data were fit using nonlinear least-squares procedures.

Time-resolved fluorescence data were obtained using an ISS K2 multifrequency and phase-modulation spectrofluorometer (Champaign, IL) equipped with an Ar-ion laser (SpectraPhysics model 2045) as the excitation source. Data were collected using the 488 nm emission line of the laser and the fluorescence emission of the porphyrin was integrated beyond 520 nm (see Jameson and Hazlett (32) for a description of phase and modulation time-resolved fluorescence methods). Emission lifetimes were extracted from the phase and modulation data using Globals Unlimited software from ISS.

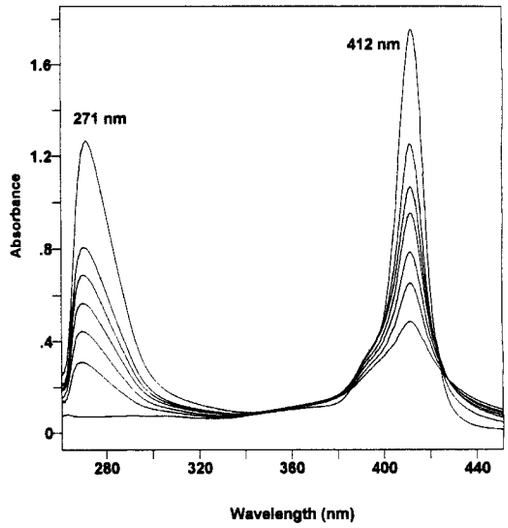

Figure 2. Optical absorption spectra of 4SP with increasing concentration of 16PC4 in the Soret region. Porphyrin concentration is 5 μ*M* in 5 m*M* potassium phosphate buffer, pH 7.0. The 16PC4 is added in 3 μ*M* increments to a final concentration of 27 μ*M* (trace with maximum absorbance at 274 nm). Spectra were obtained using a 1 cm quartz optical cuvette.

RESULTS AND DISCUSSION

Ground-state complexation

The ground-state absorption spectrum of 4SP in the presence of varying concentrations of 16PC4 in 5 m*M* potassium phosphate buffer, pH 7.0 is shown in Fig. 2. Upon addition of the 16PC4, the Soret band of 4SP (centered at 412 nm) decreases in absorbance and broadens. The difference in absorbance at 412 nm (16PC4/4SP minus 4SP) as a function of 16PC4 is plotted in Fig. 3. The solid line represents a best fit to a 1:1 stoichiometry with an association constant of (2.0 ± 0.2) × 10^5 M^{-1} using

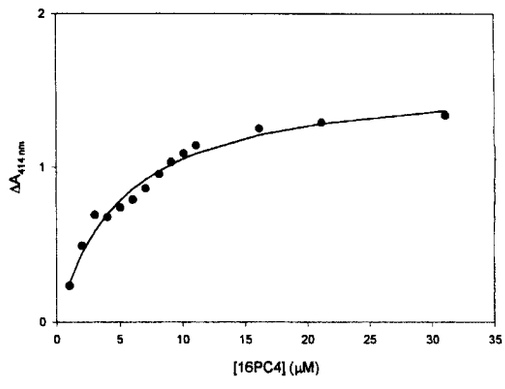

Figure 3. Plot of ΔA (412 nm) *versus* [16PC4]. The solid line is a best fit to Eq. 1 for the equilibrium: P + 16PC4 ⇌ P:16PC4.

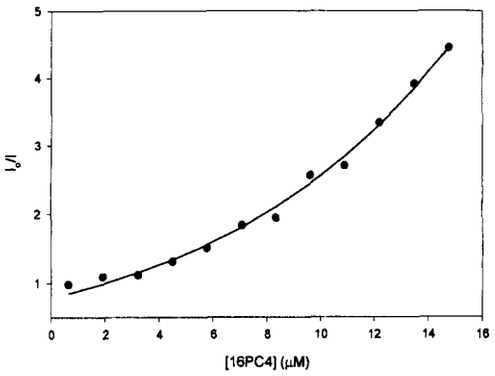

Figure 4. Stern–Volmer plot for ^{1}P in the presence of various concentrations of 16PC4. Porphyrin concentration is 5 μ*M* for 4SP. Solid line is a best fit to Eq. 2. Buffer conditions are as reported in Fig. 1.

$$\Delta A = [(1 + K_a\Delta\epsilon[16PC4])/(1 + K_a[16PC4])]P_0 \quad (1)$$

where K_a is the association constant, [16PC4] is the total concentration of added 16PC4, P_0 is the initial 4SP concentration, and $\Delta\epsilon$ is the difference in extinction coefficient between the complexed and free (also determined by the fit to be 36 ± 1.3 mM^{-1} cm^{-1}) (33). Similar titrations using the cationic T4MPYP or 4SP with higher ionic strength (0.25 *M* NaCl) did not produce any changes in the optical spectrum of the porphyrin (data not shown).

These data suggest the formation of a 1:1 electrostatically stabilized complex between 16PC4 and the 4SP. In contrast, a previous study by Firman and Wilkins (26) demonstrated that 4SP (and several metal derivatives) form electrostatically stabilized complexes with the polyammonium macrocycle [32]-$N_8H_8^{8+}$. In this case the binding occurs with a 2:1 stoichiometry and an overall association constant of 2.5 × 10^{14} M^{-1} for the first association. These authors further noted that the optical spectrum of 4SP in the presence of [32]-$N_8H_8^{8+}$ resembled that of the porphyrin alone at higher ionic strength, suggesting that the [32]ane-$N_8H_8^{8+}$ served as a template for the formation of 4SP dimers. In the present case similar optical changes are observed but the stoichiometry is clearly 1:1. It can be concluded that the optical changes observed in the 4SP:16PC4 complex arise from hydrophobic interactions between the porphyrin and the pyrimidinium rings of the 16PC4. This results in exclusion of water molecules from the interface between 4SP and 16PC4 resulting in a red shift of the visible bands. The observed stoichiometry is also consistent with charge pairing between the anionic porphyrin and the cationic macrocycle. In the case of the 4SP:[32]-$N_8H_8^{8+}$ complex the +8 charge on the ring can accommodate two 4SP (−4 charge) molecules to reach charge neutrality. In the case of the 4SP:16PC4 complex, charge neutrality is achieved with a 1:1 stoichiometry.

Singlet-state quenching

In the absence of 16PC4, 4SP fluoresces with a maximum at 620 nm and a quantum yield of 0.4. Addition of 16PC4 results in significant quenching of the singlet excited state as observed in the Stern–Volmer plot (Fig. 4). In addition, the Stern–Volmer plot exhibits pronounced upward curvature indicative of both static and dynamic quenching. Interestingly, the data could not be fit to the quadratic form of the Stern–Volmer equation, which describes both static and dynamic quenching. However, the data can be fit reasonably well to a "sphere of action" model in which

$$I_0/I = (1 + K_{SV}[16PC4])\exp(V[16PC4]) \quad (2)$$

(best-fit line in Fig. 4) where K_{SV} is the Stern–Volmer quenching constant (equal to $k_q\tau_0$) and V is the volume in which quenching takes place (34). The "sphere of action" model describes conditions in which both static and dynamic quenching occur with a range of stoichiometries (*i.e.* 1:1 plus higher order complexes). This is in contrast to the absorption data that fit to a 1:1 stoichiomery for the complex. The reason for the difference likely lies within the sensitivities of the two techniques. The dominant species, which would be prominent in the absorption spectra, appears to be that of a 1:1 complex. However, the fluorescence data (with a higher sensitivity) also detect quenching involving a smaller population of higher order ground-state complexes. Using this model and taking the lifetime of the free porphyrin as 10.03 ns (see below) the diffusional quenching rate constant (k_q) is determined to be (1.0 ± 0.5) × 10^{11} M^{-1} s^{-1}. In contrast, addition of 16PC4 to the cationic T4MPYP did not result in any significant quenching within the 16PC4 concentration range used here.

Using phase and modulation time-resolved fluorescence, the lifetime of the free porphyrin as well as the 4SP:16PC4 complex were determined. In the absence of 16PC4 the data could be fit to a single discrete component at 10.0 ns. Upon addition of 16PC4 an additional discrete component appeared with a lifetime of 1.5 ns. No other components were observed indicating no significant porphyrin degradation occurred. As with the Stern–Volmer data, addition of 16PC4 to a solution containing T4MPYP did not result in any change in lifetime of the porphyrin (5.3 ns).

Triplet-state quenching

In addition to singlet-state quenching, we also observe significant quenching of the 4SP triplet state (Fig. 5, right panel). A plot of k_{obs} (observed triplet lifetime) *versus* [16PC4] is not linear, indicating a quenching process other than simple diffusion (Fig. 6). The data could be fit to the following equation describing both diffusional and intracomplex quenching:

$$k_{obs} = [k_cK_A[16PC4]/(1 + K_A[16PC4])] + k_{trip} \quad (3)$$

where k_c is the intracomplex quenching constant, K_A is the association constant, k_{trip} is the triplet decay rate constant in the absence of quencher, and k_d is the diffusional quenching rate constant. Fitting the data for k_{obs} *versus* [16PC4] to Eq. 3 gives k_c = (1.1 ± 0.1) × 10^4 s^{-1}, k_{trip} = (2.2 ± 0.2) × 10^3 s^{-1}, and K_A = (2.4 ± 0.8) × 10^5 M^{-1}. The value obtained for k_{trip} matches that of the experimentally obtained value of (2.1 ± 0.3) × 10^3 s^{-1} within experimental error. The association constant obtained from the fit is also very near the value derived from the absorption titration ([2.4 ± 0.04] × 10^5 M^{-1} *vs* [2.0 ± 0.2] × 10^5 M^{-1}).

The model used to obtain Eq. 3 is given as follows:

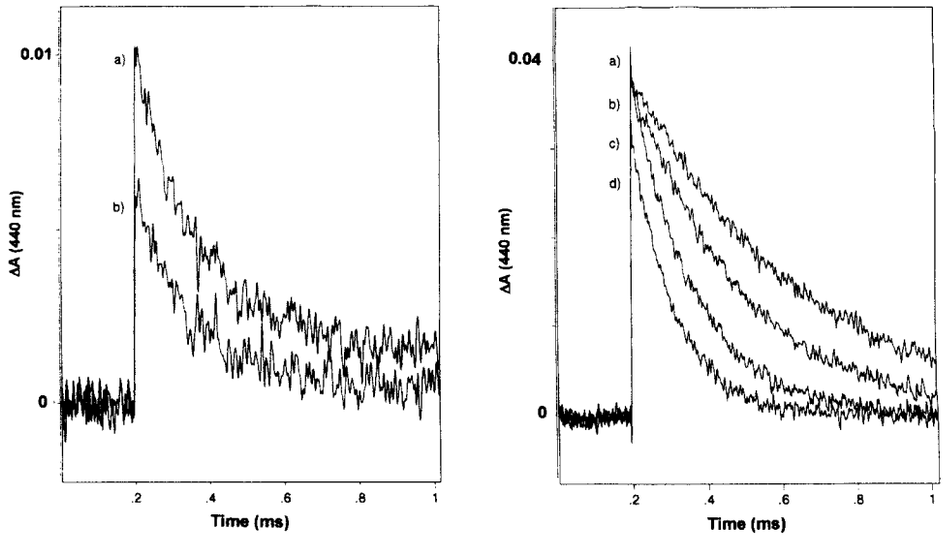

Figure 5. Left panel: Triplet-state decay of T4MPYP (10 μM) in the absence (a) and presence (b) of 16PC4. Right panel: Corresponding triplet decay of 4SP (10 μM) in the absence (trace a) and presence (traces b, 3 μM; c, 6 μM and d, 9 μM) 16PC4. Buffer conditions are as reported in Fig. 1.

$$^3P + 16PC4 \underset{k_{-1}}{\overset{k_1}{\leftrightarrow}} {}^3P{:}16PC4 \quad (4)$$

$$^3P{:}16PC4 \xrightarrow{k_c} P{:}16PC4. \quad (5)$$

In this scheme the triplet-state porphyrin forms a complex with the 16PC4 (Eq. 4) that can then undergo quenching (Eq. 5). The nature of the quenching is discussed below. The porphyrin triplet state (^3P) can undergo decay in the absence of quencher with a rate constant k_{trip}. Because the triplet lifetime data were obtained by examining the change in absorbance associated with the excited triplet state in the presence of various concentrations of 16PC4, all of the species present in the above decay scheme contribute to the overall absorbance change. Addition of 16PC4 to a solution containing T4MPYP showed no evidence of quenching (Fig. 5, left panel).

Quenching mechanism

The most probable quenching mechanism for the deactivation of either singlet-state porphyrin (^1P) or ^3P involves ET. This is due to the fact that there is no spectral overlap between the porphyrin emission (centered at 620 nm) and 16PC4 (absorption maximum near 270 nm) precluding

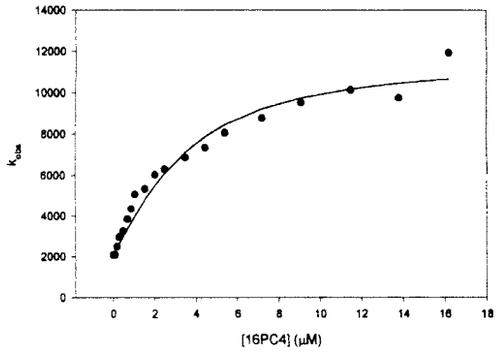

Figure 6. Plot of triplet decay rate constant *versus* [16PC4] for 4SP. Solid line is the best fit to Eq. 3. Solution conditions are the same as in Fig. 6.

quenching *via* ET. The favorablility of ET between the excited-state porphyrin and the 16PC4 can be estimated by

$$\Delta G^0 = e[E^0_{4SP} - E^0_{16PC4}] - \Delta E^* + w \quad (6)$$

where E^0_{16PC4} is the reduction potential for 16PC4, E^0_{4SP} is the reduction potential of porphyrin, ΔE^* is the energy of the excited state, e is unit electrical charge, and w is a work term for bringing together reactants and products (35). For 4SP, E^0_{4SP} = 0.86 V *versus* NHE and ΔE^* is 44.3 kcal/mol (1.92 eV) and 33.2 kcal/mol (1.44 eV) for ^1P and ^3P, respectively (30). Preliminary cyclic voltametry studies of 16PC4 in aqueous solution demonstrate a complex reduction mechanism similar to that obtained for a single pyrimidinium unit (36). The lowest potential peak appears at ~−0.15 V *versus* NHE, although the peak is quite broad. Using this value as a lower limit, the free energy for ET between the porphyrin singlet excited state and 16PC4 is ~−88 kJ/mol and for porphyrin triplet state to 16PC4 is ~−42 kJ/mol. Thus, ET from both ^1P and ^3P to the 16PC4 appears to be thermodynamically favorable.

An interesting aspect of this system is that ET from the excited porphyrin to the 16PC4 occurs with two distinct rates: a fast rate giving rise to porphyrin singlet-state quenching with a rate constant $k_s = 5.7 \times 10^8\ s^{-1}$ ($=1/\tau_q - 1/\tau_0$) and a slower rate giving rise to porphyrin triplet-state quenching with a rate constant $k_c = (1.1 \pm 0.1) \times 10^4\ s^{-1}$. The difference in rate constants could arise simply from differences in reaction driving force or from different orientations of the 16PC4 relative to the porphyrin principle axis. The ratio of two rate constants associated with ET reactions differing only in reaction driving force can be derived from semiclassical Marcus theory:

$$(k_S/k_T) = [(H^S_{AB})^2/(H^T_{AB})^2] \times \exp\{-[2\lambda(\Delta G^0_S - \Delta G^0_T) + (\Delta G^0_S)^2 - (\Delta G^0_T)^2] \div 2\lambda kT\} \quad (7)$$

where k_S/k_T is the ratio of the singlet-state ET rate constant to the triplet-state ET rate constant, H_{AB} is the electronic coupling term for the singlet/triplet-state reaction, λ is the

total reorganizational energy, k is Boltzmann's constant, T is temperature, and ΔG^0 is for the reaction origination from singlet/triplet-state quenching (37). Assuming a reasonable value for λ (1 eV) and assuming H_{AB} is the same for both singlet and triplet quenching, the ratio k_S/k_T would be ~388. However, the experimentally determined value is 5.9×10^4. Thus, the difference in rates cannot be attributed simply to the difference in reaction driving force.

This suggests that the complex forms with an equilibrium distribution of orientations with differing electronic coupling between the porphyrin and the 16PC4. The effects of orientation between donor and acceptor in nonadiabatic ET is described in the following expression for the rate constant:

$$k_{et} = (2\pi/h^2)|T_{AD}|^2FC \quad (8)$$

where FC is the sum of thermally activated Franck–Condon factors for nuclear vibration, h is Planck's constant and $|T_{AD}|^2$ is the electronic coupling matrix element that contains orientation and distance factors (38,39). An expression for T_{AD} has been given previously as

$$T_{AD} = (H_{AD} - S_{DA}H_{DD})/(1 - |S_{DA}|^2) \quad (9)$$

for a model in which the electron donor and acceptor are represented as isolated one-electron sites within oblate spheroidal potential wells. In this expression, $H_{AD} = -V_A\langle\Psi^{A*}|\Psi^D\rangle$, $H_{DD} = -V_A\langle\Psi^{D*}|\Psi^D\rangle$, and $S_{DA} = \langle\Psi^D|\Psi^A\rangle$. The wavefunctions, Ψ^A and Ψ^D, are written for an electron localized on the electron donor and acceptor, respectively, and V_A is the potential function of the acceptor. A quantitative investigation using oblate spheroid potential functions (giving wavefunctions with similar nodal characteristics as porphyrin wavefunctions) revealed the orientational dependence of ET (see Fig. 7, top). Strong coupling (*i.e.* more facile ET) between donor and acceptor was noted for geometries with $\Delta \sim 30$–$50°$ (39). In addition, when $\Delta \sim 70°$ it was predicted that the forward and back ET rates should be of comparable magnitude.

The model described above can also be applied to the 4SP:16PC4 complex (see Fig. 7, bottom). In this case the bound 4SP is represented by one ellipsoidal wavefunction and the 16PC4 represents the second ellipsoidal wavefunction. The orientational differences in ET within the 4SP:16PC4 complex can then be rationalized by qualitatively examining T_{BA}. Preliminary molecular modeling studies demonstrate two possible binding orientations. One orientation involves a face-to-face-type complex while the second involes a side-on conformation. For the singlet-state quenching the ET rate is quite facile and it is reasonable to assume that Δ and Λ are between $<\sim 30°$ and 50°. This situation is most likely to occur in the face-to-face orienation. The slower ET (*i.e.* arising from triplet-state quenching) is likely to arise from the side-on orientations because the overlap between the wavefunction on the porphyrin and the wavefunction of the 16PC4 is likely to be greatly reduced in this orientation. This would result in a significantly smaller value of T_{BA}.

Summary

The data presented here describe a novel complex between 4SP and 16PC4 with a large association constant. Photoexcitation of the complex results in ET from either ^1P or ^3P to 16PC4. In addition, no ET products are observed, suggesting facile back ET in both cases. The fact that two ET rate constants are observed within the complex suggest conformational heterogeneity. Thus, this system provides a model with which to study conformational dynamics within self-associated donor–acceptor complexes.

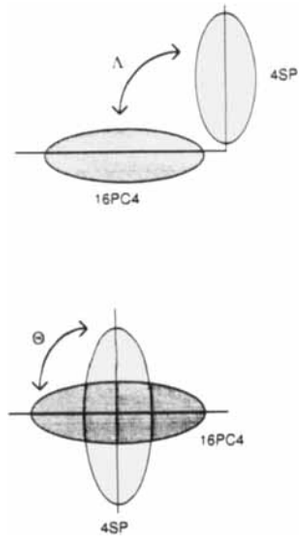

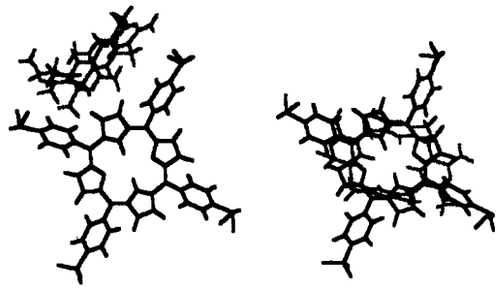

Figure 7. Top: Diagram showing orientational parameters for ET within the 4SP:16PC4 complex. See text for details. Bottom: Structural diagram of two different orientations of the 4SP:16PC4 complex. The complexes were geometry optimized using an MM+ force field with Fletcher–Reeves conjugate gradient. Energy was minimized within 0.05 kcal/mol.

Acknowledgements—The authors are indebted to Prof. Roger E. Cramer and Christopher A. Waddling for providing the 16PC4 and for invaluable discussions during the course of this work. R.W.L. also acknowledges the American Cancer Society (ACS-Institutional Seed Grant) and the American Heart Association for support of this work.

REFERENCES

1. Barbara, P. F., T. J. Meyer and M. A. Ratner (1996) Contemporary issues in electron transfer research. *J. Phys. Chem.* **100**, 13148–13168.
2. Marcus, M. A. and N. Sutin (1985) Electron transfer in chemistry and biology. *Biochim. Biophys. Acta* **811**, 265–322.
3. Boxer, S. G. (1990) Mechanisms of long-distance electron transfer in proteins: lessons from photosynthetic reaction centers. *Annu. Rev. Biophys. Biophys. Chem.* **19**, 267–299.

4. Larsson, S. (1983) Electron transfer in proteins. *J. Chem. Soc. Faraday Trans. 2* **79**, 1375–1388.
5. McLendon, G. and R. Hake (1992) Interprotein electron transfer. *Chem. Rev.* **92**, 481–490.
6. Siddarth, P. and R. A. Marcus (1990) Electron transfer reactions in proteins: a calculation of electronic coupling. *J. Phys. Chem.* **94**, 8430–8434.
7. Wuttke, D. S., M. J. Bjerrum, I-Jy Chang, J. R. Winkler, and H. B. Gray (1992) Electron tunneling in ruthenium modified cytochrome c. *Biochim. Biophys. Acta* **1101**, 168–170.
8. Isied, S. S., A. Vassilian and J. F. Wishart (1988) The distance dependence of intramolecular electron transfer rates: importance of the nuclear factor. *J. Am. Chem. Soc.* **110**, 635–637.
9. McLendon, G. (1991) *Structure and Bonding 75*, pp. 160–174. Springer-Verlag, New York.
10. Nuevo, M. R., H.-H. Chu, L. B. Vitello, and J. E. Erman (1993) Salt dependent switch pathway in the electron transfer from cytochrome c to cytochrome c peroxidase compound I. *J. Am. Chem. Soc.* **115**, 5873–5874.
11. Mauk, M. R., J. C. Ferrer and A. G. Mauk (1994) Proton linkage of complex formation between cytochrome c and cytochrome b_5: electrostatic consequences of protein–protein interactions. *Biochemistry* **33**, 12609–12614.
12. Wallin, S. A., E. D. A. Stemp, A. M. Everest, J. M. Nocek, T. L. Netzel and B. M. Hoffman (1991) Multiphasic intracomplex electron transfer from Zn cytochrome c to cytochrome c peroxidase: conformational control of reactivity. *J. Am. Chem. Soc.* **113**, 1842–1844.
13. Zhou, J. S. and N. M. Kostic (1992) Photoinduced electron transfer from zinc cytochrome c to plastocyanin is gated by surface diffusion within the metalloprotein complex. *J. Am. Chem. Soc.* **114**, 3562–3563.
14. Zhou, J. S. and N. M. Kostic (1993) Comparison of electrostatic interactions and of protein–protein orientations in electron transfer reactions of plastocyanin with the triplet state of zinc cytochrome c and with zinc cytochrome c cation radical. *Biochemistry* **32**, 4539–4546.
15. Zhou, J. S., E. S. V. Granada, N. B. Leontis and M. A. J. Rodgers (1990) Photoinduced electron transfer in self-associated complexes of several uroporphyrins and cytochrome c. *J. Am. Chem. Soc.* **112**, 5074–5080.
16. Sessler, J. L., B. Wang and A. Harriman (1993) Long-range photoinduced electron transfer in an associated but noncovalently linked photosynthetic model system. *J. Am. Chem. Soc.* **115**, 10418–10419.
17. Logunov, S. L. and M. A. J. Rodgers (1992) Self-assembled ion-pair complexes between porphyrins and bypyridinium species: picosecond dynamics of charge recombination. *J. Phys. Chem.* **96**, 8697–8700.
18. Vergeldt, F. J., R. B. Koehorst, T. J. Schaafsma, J.-C. Lambry, J.-L. Martin, D. C. Johnson and M. R. Wasielewski (1991) Subpicosecond photoinduced electron transfer in water soluble porphyrin dimers. *Chem. Phys. Lett.* **107**, 107–113.
19. Brun, A. M., A. Harriman and S. J. Hubig (1992) Laser spectroscopy of porphyrin–azaaromatic ion pairs: influence of molecular dimensions on the rate of charge recombination. *J. Phys. Chem.* **96**, 254.
20. Tecilla, P., R. P. Dixon, G. Slobodkin, D. S. Alavi, D. H. Waldeck and A. D. Hamilton (1990) Hydrogen bonding self-assembly of multichromophore structures. *J. Am. Chem. Soc.* **112**, 9408–9410.
21. Turro, C., C. K. Chang, G. E. Leroi, R. I. Cukier and D. G. Nocera (1992) Photoinduced electron transfer mediated by a hydrogen-bonded interface. *J. Am. Chem. Soc.* **114**, 4013–4015.
22. Jasuja, R., D. M. Jameson, C. K. Noshijo and R. W. Larsen (1997) Singlet excited state dynamics of tetrakis(4-*N*-methylpyridyl)porphine associated with DNA nucleotides. *J. Phys. Chem. B* **101**, 1444–1450.
23. Larsen, R. W., D. H. Omdal, R. Jasuja, S. L. Niu and D. M. Jameson (1997) Conformational modulation of electron transfer within electrostatic porphyrin : cytochrome *c* complexes. *J. Phys. Chem. B* **101**, 8012–8020.
24. Larsen, R. W., R. Jasuja, S. L. Niu and K. Dwivedi (1997) Ground and excited state characterization of self-assembled Ru(II)-tris-bipyridine–iron porphyrin complexes. *Photochem. Photobiol. Sect. A* **107**, 71–75.
25. Manfrin, M. F., L. Moggi, V. Castelvetro, M. Balzani, M. W. Hosseini and J. M. Lehn (1985) Control of the photochemical reactivity of coordination compounds by formation of supramolecular structures: the case of the hexacyanocobalt(III) anion associated with polyammonium macrocycle receptors. *J. Am. Chem. Soc.* **107**, 6888–6892.
26. Firman, P. and R. G. Wilkins (1985) Induced dimerization of tetrakis (*p*-sulphonatophenyl)porphine and metallo-derivatives by a polyammonium macrocycle [32]-$N_8H_8^{8+}$. *J. Am. Chem. Soc.* **111**, 4990–4992.
27. Chandrashekar, T. K., H. Willigen and M. H. Ebersole (1984) Optical and electron spin resonance study of cation and cation-crown ether induced dimerization of tetrakis(4-sulphonatophenyl)porphyrin. *J. Phys. Chem.* **88**, 4326–4332.
28. Rampi, M. A., M. T. Indelli, F. Scandola, F. Pina, and A. J. Parola (1996) Photophysics of supercomplexes. Adduct between $Ru(bpy)(CN)_4^{2-}$ and the [32]ane-$N_8H_8^{8+}$ polyaza macrocycle. *Inorg. Chem.* **35**, 3355–3361.
29. Cramer, R. E., V. Fermin, E. Kuwabara, R. Kirkup, M. Selman, K. Aoki, A. Adeyamo and H. Yamazaki (1991) Synthesis and structure of the chloride and nitrate inclusion complex of [16-pyrimidinium crown-4]$^{4+}$. *J. Am. Chem. Soc.* **113**, 7033–7034.
30. Kalyanasundaram, K. and M. Neumann-Spellart (1984) Photophysical and redox properties of water soluble porphyrins in aqueous media. *J. Phys. Chem.* **86**, 5163–5169.
31. Larsen, R. W., J. Murphy and E. W. Findsen (1996) Structure and dynamics of CO–iron(II) protoporphyrin IX in dimethyl sulphoxide. *Inorg. Chem.* **35**, 6254–6260.
32. Jameson, D. M. and T. L. Hazlett (1991) Time-resolved fluorescence measurements in biology and biochemistry. In *Biophysical and Biochemical Aspects of Fluorescence Spectroscopy* (Edited by T. G. Dewey). Plenum Press, New York.
33. Connors, K. A. (1987) *Binding Constants: The Measurement of Molecular Complex Stability*. John Wiley and Sons, New York.
34. Laws, W. and P. B. Contino (1992) Fluorescence quenching studies: analysis of nonlinear Stern–Volmer data. *Methods. Enzymol.* **210**, 448–463.
35. Rehm, D. and A. Weller (1970) Kinetics of fluorescence quenching by electron and H-atom transfer. *Isr. J. Chem.* **8**, 259–271.
36. Elving, P. J., S. J. Pace and J. E. O'Reilly (1973) Electrochemical reduction of purine, pyrimidine, and imidazole in aqueous media: kinetics and mechanism. *J. Am. Chem. Soc.* **95**, 647–658.
37. Schmidt, J. A., A. R. McIntosh, A. C. Weedon, J. R. Bolton, J. S. Connolly, J. K. Hurley and M. R. Wasielewski (1988) Intramolecular photochemical electron transfer. 4. Singlet and triplet mechanisms of electron transfer in a covalently linked porphyrin-amide-quinone molecule. *J. Am. Chem. Soc.* **110**, 1733–1740.
38. Cave, R. J., P. Siders and R. A. Marcus (1986) Mutual orientation effects on electron transfer between porphyrins. *J. Phys. Chem.* **90**, 1436–1444.
39. Siders, P., R. J. Cave and R. A. Marcus (1984) A model for orientation effects in electron transfer reactions. *J. Chem. Phys.* **81**, 5613–5624.